Title
Substrate control in stereoselective lanthionine biosynthesis.

Journal
Nature chemistry, 7(1)

ISSN
1755-4330

Authors
Tang, Weixin
Jiménez-Osés, Gonzalo
Houk, KN
et al.

Publication Date
2015

DOI
10.1038/nchem.2113

Peer reviewed

HHS Public Access

Author manuscript

Nat Chem. Author manuscript; available in PMC 2015 July 01.

Published in final edited form as:

Nat Chem. 2015 January ; 7(1): 57–64. doi:10.1038/nchem.2113.

Substrate Control in Stereoselective Lanthionine Biosynthesis

Weixin Tang[1], **Gonzalo Jiménez-Osés**[2], **K. N. Houk**[2,*], and **Wilfred A. van der Donk**[1,*]

[1]Department of Chemistry and Howard Hughes Medical Institute, University of Illinois at Urbana-Champaign, Urbana, Illinois 61801, USA

[2]Department of Chemistry and Biochemistry, University of California, Los Angeles, Los Angeles, CA 90095-1569, USA

Abstract

Enzymes are typically highly stereoselective catalysts that enforce a reactive conformation on their native substrates. We report here a rare example where the substrate controls the stereoselectivity of an enzyme-catalyzed Michael-type addition during the biosynthesis of lanthipeptides. These natural products contain thioether crosslinks formed by cysteine attack on dehydrated Ser and Thr residues. We demonstrate that several lanthionine synthetases catalyze highly selective *anti* additions in which the substrate (and not the enzyme) determines whether the addition occurs from the *Re* or *Si* face. A single point mutation in the peptide substrate completely inverted the stereochemical outcome of the enzymatic modification. Quantum mechanical calculations reproduced the experimentally observed selectivity and suggest that conformational restraints imposed by the amino acid sequence on the transition states determine the face selectivity of the Michael-type cyclization.

The stereochemical outcome of chemical reactions between chiral molecules in which one or more new stereocenters are generated is often governed by the stereochemistry of the substrate or reagent, resulting in substrate or reagent controlled processes[1]. For enzymatic reactions, the well-organized chiral environment of the enzyme active site typically results in reagent control for physiological processes. In this study, we discovered a rare case where the substrate controls the stereochemical outcome of an enzyme-catalyzed Michael-type addition during the biosynthesis of lanthipeptides.

Lanthipeptides are a large family of ribosomally synthesized and post-translationally modified peptides (RiPPs), which constitute a growing class of natural products[2]. Their

*To whom correspondence should be addressed: Wilfred A. van der Donk, 600 S. Mathews Avenue, Urbana, Illinois 61801, United States; vddonk@illinois.edu; phone: (217) 244-5360; fax: (217) 244-8533. K.N. Houk, Department of Chemistry and Biochemistry, University of California, Los Angeles, California 90095-1569, United States; houk@chem.ucla.edu; phone: (310) 206-0515; fax: (310) 206-1843.

Author Contributions

W.T. and W.A.v.d.D. designed the study. W.T. performed all experiments. G.J.O. performed all the theoretical studies. W.T., G.J.O., K.N.H. and W.A.v.d.D. analyzed the data and wrote the manuscript.

Competing financial interests

The authors declare no competing financial interests.

precursor peptides (called LanAs) consist of an N-terminal leader peptide that is essential for recognition by the enzymes that carry out the post-translational modifications[3] (Fig. 1a). The latter take place in the C-terminal core region of the precursor peptide, and involve dehydration of serine and threonine residues to generate dehydroalanine (Dha) and dehydrobutyrine (Dhb), respectively (Fig. 1a and 1b). Subsequently, the thiols from cysteine residues are added to the newly formed double bonds in Dha and Dhb via a Michael-type addition. The resulting thioether bridges are termed lanthionine (Lan) and methyllanthionine (MeLan), respectively (Fig. 1b). In class II lanthipeptides, both the dehydration and cyclization reactions are catalyzed by one bi-functional enzyme that is generically termed LanM (e.g. CylM in Fig. 1a)[4,5]. Many lanthipeptides display antimicrobial activity and are designated lantibiotics[6], with some members potently inhibiting the growth of a broad range of pathogens[7].

Lanthipeptides have been extensively studied over the past 30 years, with structural information available for a subset of compounds[8]. Until recently, it was generally assumed that the cysteine addition always gave (2*S*, 6*R*)-Lan (hereafter called DL-Lan) and (2*S*, 3*S*, 6*R*)-MeLan (hereafter DL-MeLan) (Fig. 1b). This assumption was recently challenged by the discovery of (2*R*, 3*R*, 6*R*)-MeLan (LL-MeLan, Fig. 1b) in two class II lantibiotics - the cytolysin from *Enterococcus faecalis* and haloduracin produced by *Bacillus halodurans*[9]. The enterococcal cytolysin consists of two peptides called cytolysin L ($CylL_L$", Figure 1c) and cytolysin S ($CylL_S$", Figure 1a), which are generated from the precursor peptides $CylL_L$ and $CylL_S$, respectively, by a single lanthionine synthetase CylM. The production of cytolysin enhances virulence in infection models of *E. faecalis* and is associated with acute patient mortality[10–13]. Haloduracin is an antimicrobial substance that also consists of two peptides (Fig. 1c)[14]. Based on sequence homology of the rings containing the LL-MeLan residues in cytolysin and haloduracin, we have suggested that a Dhb-Dhb-Xxx-Xxx-Cys motif (Xxx represents amino acids other than Dha, Dhb and Cys) (Fig. 1) induces the formation of the unusual MeLan stereochemistry[9]. In this model, the LL stereochemistry is formed by *anti*-addition of cysteine to the *Re* face of the alkene because of a conformational preference of the substrate that is unique to this motif[9].

These findings have raised a number of intriguing questions. First, given that cytolysin and haloduracin contain both LL- and DL-(Me)Lan, how can one enzyme catalyze similar conjugate additions with different stereochemistries in a single polypeptide substrate? Second, does the substrate sequence indeed govern the diastereoselectivity? And third, is it possible to manipulate the stereochemical outcome by mutating the peptide substrate? In this study, we show that the formation of LL-MeLan from the Dhb-Dhb-Xxx-Xxx-Cys sequence is not specific to the enzymes involved in cytolysin or haloduracin biosynthesis. Furthermore, we demonstrate that a Dhb-to-Ala mutation at the second position of the motif results in MeLan formation with the canonical DL stereochemistry, supporting the substrate control hypothesis. Quantum mechanical simulations of dehydrated peptides confirm an intrinsic preference for *Re* face or *Si* face addition depending on the sequence of the substrate peptide.

Results

Generality of LL-MeLan formation from Dhb-Dhb-Xxx-Xxx-Cys

To test the hypothesis that the substrate peptide sequence containing the Dhb-Dhb-Xxx-Xxx-Cys motif determines the formation of LL stereochemistry independent of the identity of the lanthionine synthetase, we generated chimeric peptides with the $CylL_S$ core peptide connected to leader peptides from different class II lanthipeptides. These leader peptides were expected to be recognized by their cognate lanthionine synthetases that carry out the dehydration and cyclization reactions in the core peptide (Fig. 2a). The gene *halA2-cylL*$_S$ that encodes a chimeric peptide consisting of the leader peptide of the haloduracin β (Halβ) precursor peptide (HalA2) fused to the $CylL_S$ core peptide (Fig. 2a) was co-expressed in *E. coli* with *halM2* encoding the Halβ synthetase HalM2[15]. Modified HalA2-$CylL_S$ was purified and analysis by matrix-assisted laser desorption ionization time-of-flight (MALDI-TOF) mass spectrometry (MS) showed the desired four dehydrations (Supplementary Results, Supplementary Fig. S1). The modified chimeric peptide was hydrolyzed in 6 M HCl to individual amino acid residues, which were derivatized and analyzed by gas chromatography (GC) MS using a chiral GC column to reveal the stereochemistry of the (Me)Lan residues[9,16]. Signals corresponding to LL-MeLan and DL-Lan were observed as the predominant products by comparison with synthetic standards derivatized in the same way (Fig. 2b, 2c; Table 1 and Supplementary Fig. S2). Hence, HalM2 catalyzes the cyclization of the $CylL_S$ core peptide with the same stereochemical selectivity as CylM. This result was perhaps not too surprising since HalM2 converts a Dhb-Dhb-Trp-Pro-Cys sequence into an LL-MeLan cross-link in its native substrate HalA2 (Fig. 1c)[9]. We therefore turned to LanM enzymes that only form DL-(Me)Lan in their natural substrates. The lanthionine synthetase LtnM2 involved in the biosynthesis of the lantibiotic lacticin 3147 A2[17] was evaluated next. An LtnA2-$CylL_S$ peptide consisting of the leader peptide from the natural LtnM2 substrate (LtnA2) and the core peptide from $CylL_S$ was co-expressed with LtnM2 in *E. coli*. MALDI-TOF MS analysis illustrated the desired four dehydrations (Supplementary Fig. S3). Hydrolysis and derivatization of the modified LtnA2-$CylL_S$ peptide once again resulted in almost exclusive LL-MeLan and DL-Lan signals in GC-MS experiments (Fig. 2b, 2c; Table 1 and Supplementary Fig. S4), demonstrating that LtnM2 also preferentially forms the LL stereochemistry when guided by the substrate sequence. We then chose ProcM as our next LanM target. ProcM is a lanthionine synthetase with 29 natural substrates (ProcAs) that exhibits high substrate tolerance[18]. ProcM can generate many different ring topologies, and based on the currently structurally characterized ProcA products, they all have the DL-(Me)Lan stereochemistry (Supplementary Fig. S5)[19]. It has been suggested that it is the sequence of the ProcA peptides, rather than the ProcM enzyme, that primarily determines the cyclization patterns[20]. As such, ProcM would be the perfect candidate to test the hypothesis that the unusual LL-MeLan stereochemistry produced from the Dhb-Dhb-Xxx-Xxx-Cys motif is determined by the substrate. In this study, the ProcA3.2 leader peptide was chosen for a chimeric ProcA3.2-$CylL_S$ peptide and the latter was co-expressed with ProcM in *E. coli*. The modified ProcA3.2-$CylL_S$ peptide afforded several products that differed in the extent of dehydration with 2- and 4-fold dehydrated peptides as the major products (Supplementary Fig. S6). The modified peptides were hydrolyzed, and the resulting amino acids were derivatized and subjected to GC-MS analysis. In this case,

we observed an LL-MeLan peak with a relatively low intensity as well as a DL-Lan signal (Fig. 2b, 2c; Table 1 and Supplementary Fig. S7). The low signal intensity of the derivatized MeLan compared with Lan could be the result of the observed incomplete dehydration of the non-cognate core peptide or because of partial cyclization by ProcM. Regardless, the MeLan that was generated clearly was formed with high selectivity for the LL stereochemistry. Collectively, these results demonstrate that class II LanM enzymes have a general preference for converting sequences containing the Dhb-Dhb-Xxx-Xxx-Cys motif into LL-MeLan (Table 1).

Mutation of the Dhb-Dhb-Xxx-Xxx-Cys motif

To probe whether the two consecutive dehydro amino acids in the motif impart formation of the LL stereochemistry, Thr2 in HalA2 was mutated to Ala. The HalA2-T2A peptide was co-expressed with its synthetase HalM2 in *E. coli*, resulting in the desired elimination of six water molecules. After leader peptide removal via an engineered Factor Xa cleavage site[15], the modified HalA2-T2A core peptide was subjected to tandem MS (MS/MS) analysis, which confirmed the formation of the expected ring pattern (Fig. 3a). The modified peptide was then hydrolyzed, and the resulting amino acids were derivatized and analyzed by GC-MS. A DL-MeLan signal was almost exclusively observed, compared with a 2:1 ratio of DL:LL MeLan signals observed for the wild-type HalA2 peptide after HalM2 modification (the LL-MeLan residue originating from the A ring and two DL-MeLan residues originating from the C and D rings) (Fig. 3b, Table 1 and Supplementary Fig. S8)[9]; as expected the DL-configuration of the Lan residue (ring B) remained unchanged in the mutant (Supplementary Fig. S8). To rule out the possibility that the A ring of the HalA2-T2A mutant was not properly cyclized, which would mean that the observed DL-MeLan signal originated solely from the C and D rings, we used trypsin to remove the leader peptide and analyzed the core peptide mass with liquid chromatography MS (LC-MS). If the A ring of the HalA2-T2A mutant was not properly cyclized, the core peptide would start with a Dhb, which would hydrolyze to a ketone after the removal of the leader peptide, giving a mass increase of 1 Da[14]. We chose trypsin over Factor Xa because trypsin exhibits minimal bias in terms of digestion efficiency when the cleavage site is located next to a dehydrated amino acid[21]. The observed mass for the HalA2-T2A core peptide was 2318.0476 Da (Fig. 3c), in agreement with the calculated mass of the cyclized peptide (2318.0469 Da). We did not observe any peak in the LC trace with a mass corresponding to the non-cyclized peptide (calculated 2319.0309 Da). Collectively, these results show that the A ring of the HalA2-T2A mutant was successfully cyclized and had the DL stereochemistry, strongly suggesting that the 2nd Dhb in the Dhb-Dhb-Trp-Pro-Cys sequence is critical for the formation of LL-MeLan by HalM2. By mutation of the 2nd Dhb to Ala, the stereochemistry of the MeLan residue in the A ring of HalA2 could be successfully changed from LL to DL.

Computational studies on the inherent cyclization stereoselectivity

Computational simulations have been successfully applied previously to correlate inherent substrate reactivity with observed enzymatic selectivities[22,23]. To investigate the possible origins of the experimentally observed sequence-dependent stereochemical preferences in this work, the cyclization reactions were studied computationally for the A rings of the $CylL_S$ and HalA2 core peptides. The high flexibility of the substrates confers the stereo-

determining transition structures (TS) a potentially vast conformational diversity; therefore, a multilevel approach combining molecular dynamics (MD) and quantum mechanical (QM) calculations of optimized TS was employed to locate the minimum energy pathways for both *Re* and *Si* face additions for each model peptide.

The $CylL_S$ sequence leading to its A ring was very rigid in the MD simulations (Fig. 4a) as depicted by the Ramachandran plots of the residues involved in the macrocyclization (Fig. 4b–f). In the experimentally favored *Re*-face approach, the Dhb-Dhb and Pro-Ala sequences act synergistically to generate a stable secondary structure with characteristics of both α-helix (*i*+4→*i* hydrogen bonding) and 3_{10}-helix (*i*+3→*i* hydrogen bonding), as previously found for peptides containing α,β-dehydro amino acids[24,25]. The majority of the Cys population (64%) was also found in a helix-like secondary structure, whereas the non-reactive Dhb attained a distorted γ-turn-like arrangement in which the α,β-unsaturated carbonyl system deviates from planarity due to hydrogen bonding interactions and the influence of the neighboring proline. Well-defined hydrogen bonds between the carbonyl of the reactive Dhb and the amide hydrogens of Ala (*i*+3) and Cys (*i*+4) were observed along the entire MD trajectory. Additional hydrogen bonds between the carbonyl of the adjacent Dhb (*i*+1) and the amide hydrogens of Ala and Cys further stabilize this tightly folded motif. In contrast, the secondary structure of the $CylL_S$ A-ring sequence for *Si* face approach is more flexible. In order for the nucleophilic cysteine to approach the *Si* face of the alkene, the reactive Dhb changes from an α-helical (*s-cis*) to a PPII (*s-trans*) conformation (the latter having two mirror image populations, Figure 4b), forced by the rigidity of the proline backbone. This proline is in α-helix and PPII conformations in a 70:30 ratio, and the adjacent Dhb is also flexible, showing two main populations with γ-turn (distorted *s-trans*, 72%) or α_L-helix-like (distorted *s-cis*, 23%) conformations. The four hydrogen bonds described above are frequently disrupted, which correlates with transitions between the described conformations (Supplementary Fig. S9). Overall, this higher flexibility and the disruption of the tight hydrogen bond network suggest that the *Si* face approach might be disfavored for the Dhb-Dhb-Pro-Ala-Cys sequence.

These preliminary observations were confirmed by the large difference in the activation barriers ($\Delta\Delta G^{\ddagger}$) calculated for the Michael-type additions to the *Re* and *Si* faces of Dhb, which favors the diastereoselective formation of LL-MeLan by 3.2 kcal mol^{-1} (>99:1 *d.r.* at 25 °C, Supplementary Table 2), in agreement with our experimental observations (Table 1 and Fig. 5). This preference for the *Re* face approach is rationalized in terms of the ability of the substrate to form a rigid oxyanion hole in this orientation (Fig. 5), allowing efficient stabilization of the incipient negative charge on the carbonyl oxygen by two amide hydrogens. Of note, the backbone amides stabilize the enolate sufficiently to make the nucleophilic attack slightly exergonic, which is not the normal trend for thio-Michael additions in solution[26]. Additionally, in the favored *Re* face approach, the enamide is in the more reactive *s-cis* conformation, which may further stabilize the corresponding TS compared to that of the *Si* face approach, in which the enamide is in a less reactive *s*-trans conformation[26].

The shift of the proline from the *i*+2 to the *i*+3 position with respect to the reacting Dhb, as found in the HalA2 sequence (Dhb-Dhb-Trp-Pro-Cys), completely changes the secondary

structure in both reactive trajectories (Supplementary Fig. S10). In the *Re* face approach, the reacting Dhb still exhibits an α-helical conformation (planar *s-cis*), but the non-reacting Dhb and Pro adopt mainly an inverse PPII conformation (planar *s-trans*) due to the release of conformational constraints imposed in $CylL_S$ by the neighboring proline and the hydrogen bond network. The ability to attain a 3_{10}-helix is seriously hampered by the impossibility to establish $i+3 \rightarrow i$ hydrogen bonds with the reacting Dhb, and therefore the intricate hydrogen bond pattern described above for the $CylL_S$ sequence is lost. The secondary structure for the *Si* face approach is similar, with no persistent hydrogen bonds along the simulation. Unlike in $CylL_S$, the approach of the cysteine to the *Si* face of Dhb in HalA2 is achieved by maintaining the reactive Dhb in an α-helical type conformation and isomerizing the neighboring Dhb from a PPII (*s-trans*) to an α-helical (*s-cis*) conformation. However, the most stable TS for the Michael-type addition differ from those sampled preferentially in the restrained MD for the neutral cysteine (Supplementary Fig. S11). Notably, the lowest energy conformations of the two Dhb residues in the TS are completely reversed from those calculated for the $CylL_S$ sequence: *s-trans* for the reacting Dhb and *s-cis* for the adjacent Dhb in the *Re* face approach, and *s-cis* for both Dhb residues in the *Si* face approach. Nevertheless, very high stereoselectivity (96:4, see Supplementary Table 2) towards LL-MeLan formation was calculated for this sequence based upon the transition state energies, in agreement with the experiments. It should be noted that the HalA2 sequence does not allow the formation of the tight oxyanion hole observed for $CylL_S$. Consequently, the thio-Michael addition shows the normal endergonic behavior yielding a higher energy enolate, with the overall transformation becoming favored only upon protonation. Interestingly, the HalA2 sequence confers the necessary conformational bias to override the suggested less reactive character of the *s-trans* enamide for the favored *Re* approach[26].

With the intrinsic preference for the *Re* face addition established in the A rings of both cytolysin S and Halβ, we next investigated the reversal of stereochemistry in the HalA2-T2A mutant. The secondary structure of the A-ring sequence of the mutant is quite similar to that of HalA2 (Supplementary Fig. S10 & S12), but the mutation has a deep impact on the calculated stereoselectivity, favoring the *Si* face approach by 2 kcal mol^{-1} in line with the experimental observations. Intriguingly, the geometries of the lowest energy TS calculated for this sequence are virtually identical to those of the wild-type sequence, but the stereoselectivity is reversed (Table 1 and Supplementary Fig. S13). The presence of an sp^3-hybridized alpha carbon in the Ala instead of the planar arrangement in Dhb perturbs the peptide backbone very slightly, but enough to alter the electrostatic environment of the reacting fragments. This change is reflected in the molecular dipole moments (μ) calculated for the lowest energy TS; whereas in HalA2, the TS for *Re* face approach is slightly more polar (μ = 12.6 D) than for the *Si* face approach (μ = 11.6 D), for HalA2-T2A both TS are equally polar (μ = 13.7 D and 13.6 D for *Re* and *Si* face approaches, respectively). In the absence of the strong structural driving forces observed for $CylL_S$, more polar TS will be preferentially stabilized in moderately polar environments such as the continuum solvent used in the calculations and as found in protein active sites, and this is indeed observed for HalA2. However, when both TS are equally polar as in HalA2-T2A, the intrinsically more reactive character of the enamide *s-cis* conformation in the *Si* face approach appears to result in reversal of the stereoselectivity with respect to HalA2. Overall, these striking results

reflect the complexity of the factors that govern the facial selectivity in the biosynthesis of lanthipeptides, since dissimilar sequences with significantly different three-dimensional arrangements can provide the same stereoselectivity, but a very subtle change in the sequence with almost no geometric effect completely reverts the face selectivity. These stereodetermining structural preferences were calculated to be intrinsic to the oligopeptide sequences consistent with the observation that the stereochemical outcome is independent of the lanthionine synthetases used.

Discussion

The discovery of LL-MeLan residues in the enterococcal cytolysin and haloduracin formed from a conserved Dhb-Dhb-Xxx-Xxx-Cys substrate motif revealed the first examples of enzymatic formation of non-canonical stereochemistry of MeLan residues. Very recently, LL stereochemistry was also reported for the lantibiotic carnolysin that also contains this motif[27]. We show in this work that the unusual stereochemistry is inherent to this sequence motif, because four different class II lanthionine synthetases with low sequence identities in their cyclase domains (<25% identity) all converted this motif to LL-MeLan products even though the enzymes install other rings in the same peptide with DL stereochemistry. Indeed, two of the tested lanthionine synthetases only give products with DL stereochemistry in their natural substrates, making it highly unlikely that they would have evolved features that favor LL-MeLan-containing products. Furthermore, the stereoselectivity was changed from LL to DL when the second Dhb in such a motif in HalA2 was mutated to Ala. Thus, these Michael-type additions are rare examples of natural enzymatic processes in which stereochemistry is substrate-controlled; we have not been able to find other such examples, but a related observation has been made in ketoreduction by iterative polyketides synthases where substrate length controlled the face selectivity of hydride transfer[28]. Of course, reversal of stereoselectivity of enzymatic reactions has been observed routinely with non-natural substrate analogs or mutant enzymes[29–32].

The computational studies also support a model in which the observed stereochemistry is determined to a large extent by the sequence of the substrate peptide, even though the transition state structures can differ substantially depending on the location of a Pro residue. We suggest that for the formation of most (Me)Lan residues in lanthipeptides, the enzyme controls the face selectivity of attack and protonation, resulting in the predominantly observed DL stereochemistry. However, we hypothesize that two consecutive Dhb residues in the Dhb-Dhb-Xxx-Xxx-Cys motif result in a conformational preference that is unfavorable for the canonical interaction with the enzyme active site. The enzyme is likely to still activate the Cys residue given the very slow rates of non-enzymatic (Me)Lan formation[33], but the face selectivity of attack is now governed by the substrate and not the enzyme. The role of the enzyme might be investigated in more detail if the cyclization reaction could be decoupled from the dehydration reaction such that the non-enzymatic reaction could be studied in isolation. Structural information of substrate bound to the enzyme will be required to determine whether all calculated transition states can be attained in the context of the protein; at present no structures of LanM enzymes are available.

Methods

General methods

All polymerase chain reactions (PCR) were carried out on a C1000™ thermal cycler (Bio-Rad). DNA sequencing was performed by ACGT, Inc. MALDI-TOF MS was carried out on a Bruker Daltonics UltrafleXtreme MALDI TOF/TOF instrument (Bruker). LC-ESI-Q/TOF MS and MS/MS analyses were conducted using a Synapt G1 instrument with an Acquity UPLC system (Waters), which was equipped with a Jupiter Proteo C12 column (5 μm; 90 Å; 100 × 1.0 mm) (Phenomenex). GC-MS analysis was performed in the Mass Spectrometry Laboratory (School of Chemical Sciences, UIUC) on an Agilent 7890 gas chromatograph (Agilent) with a CP-Chirasil-L-Val fused silica column (25 m × 0.25 mm × 0.15 μm) (Agilent). Solid phase extraction was performed with Strata-X polymeric reverse phase columns (Phenomenex).

Materials

All oligonucleotides were obtained from Integrated DNA Technologies and used as received. Restriction endonucleases, DNA polymerases, and T4 DNA ligase were purchased from New England Biolabs. Media components were obtained from Difco Laboratories. Trypsin was purchased from Worthington Biochemical Corporation; Factor Xa was obtained from New England Biolabs and other endoproteinases were ordered from Roche Biosciences.

Strains and plasmids

E. coli DH5α and *E. coli* BL21 (DE3) cells were used as host for cloning and plasmid propagation, and host for protein expression, respectively. Co-expression vector pRSFDuet-1 was obtained from Novagen.

Construction of plasmids and expression of peptides

See the method section in the Supplementary Information.

GC-MS analysis

The synthesis of Lan and MeLan standards and the preparation of samples for GC-MS analysis were carried out following a reported procedure published elsewhere[16,19]. The modified full length peptides with their leader peptides attached were hydrolyzed and the resulting solutions were dried and directly used for derivatization. The derivatized samples were analyzed by GC-MS using an Agilent 7890 gas chromatograph equipped with a CP-Chirasil-L-Val fused silica column (25 m × 0.25 mm × 0.15 μm). Samples were dissolved in methanol and introduced to the instrument via a split (1:20) injection at a flow rate of 1.7 mL/min helium gas. The temperature method used was 160 °C for 2 min, 160 °C to 180 °C at 3 °C/min, and 180 °C for 2 min. The selected-ion monitoring (SIM) was achieved by extracting the total ion spectra for peaks containing the characteristic fragment masses of 365 Da for Lan and 379 Da for MeLan residues.

Protease cleavage of the leader peptides

Modified HalA2-CylL$_S$, ProcA3.2-CylL$_S$ and HalA2-T2A peptides were dissolved in H_2O to a concentration of 3 mg/mL. To a total 200 μL reaction with a final peptide concentration of 200 μM, 20 μL of 500 mM HEPES buffer (pH 7.5) was added, followed by 10 μL of 0.02 mg/mL AspN protease (for HalA2-CylL$_S$), 1 mg/mL GluC protease (for ProcA3.2-CylL$_S$), and 1 mg/mL Factor Xa or 5 mg/mL trypsin (for HalA2-T2A). The protease cleavage reactions were incubated at 25 °C for 6 to 16 h.

LC-ESI-Q/TOF MS and MS/MS analysis

LC-ESI-Q/TOF MS and MS/MS analysis were performed on a Waters Synapt G1 mass spectrometer. For detailed instrument settings, experimental conditions, and data analysis, see the method section in the Supplementary Information.

MD simulations

Constrained MD simulations in water were performed using the AMBER 12 package (Case, D. A. et al., UCSF, 2012). Parameters for non-natural dehydro amino acids were generated using the general AMBER force field (*gaff*)[35], with partial charges set to fit the electrostatic potential generated at the HF/6-31G(d) level by the RESP model[36]. Water molecules were treated with the SHAKE algorithm. Long-range electrostatic effects were modeled using the particle-mesh-Ewald method[37]. An 8 Å cutoff was applied to Lennard-Jones and electrostatic interactions. The Langevin equilibration scheme was used to control and equalize the temperature with a 2 fs time step at a constant pressure of 1 atm and temperature of 300 K. Production trajectories were run for 100 ns using McCammon's accelerated MD (aMD) algorithm[38,39].

DFT calculations

All calculations were carried out with the Gaussian 09 package (Frisch, M. J. *et al.*, Gaussian, Inc., 2009). Full geometry optimizations and transition state searches were carried out with the ω-B97X-D range-separated hybrid functional[40] and 6-31G(d) basis set. Frequency analyses were carried out at the same level used in the geometry optimizations. Single point energies were calculated with the M06-2X hybrid functional[41] on the optimized geometries. Bulk electrostatic effects were considered implicitly during optimization and energy evaluation through the IEF-PCM polarizable continuum model[42]. Cartesian coordinates, electronic energies, entropies, enthalpies, Gibbs free energies and lowest frequencies of the low energy conformations are available in Supplementary Table 2. For details of the computational studies, see the method section in the Supplementary Information.

Supplementary Material

Refer to Web version on PubMed Central for supplementary material.

Acknowledgments

We thank Dr. M. Carmen Martínez-Cuesta for providing the pBAC105 plasmid encoding LtnM2 from *Lactococcus lactis* IFPL105 and Dr. Leigh Anne Furgerson for constructing the pET15b-HalA2-T2A plasmid. We thank Furong

Sun for assistance with GC-MS analysis. This work was supported by the National Institutes of Health (GM 58822 to W.v.d.D. and GM 075962 to K.N.H.). Calculations were performed on the Hoffman2 cluster at UCLA and the Extreme Science and Engineering Discovery Environment (XSEDE), which is supported by the National Science Foundation (OCI-1053575).

References

1. Masamune S, Choy W, Petersen JS, Sita LR. Double asymmetric synthesis and a new strategy for stereochemical control in organic synthesis. Angew. Chem. Int. Ed. Engl. 1985; 24:1–30.
2. Arnison PG, et al. Ribosomally synthesized and post-translationally modified peptide natural products: overview and recommendations for a universal nomenclature. Nat. Prod. Rep. 2013; 30:108–160. [PubMed: 23165928]
3. Yang X, van der Donk WA. Ribosomally synthesized and post-translationally modified peptide natural products: new insights into the role of leader and core peptides during biosynthesis. Chem.-Eur. J. 2013; 19:7662–7677. [PubMed: 23666908]
4. Siezen RJ, Kuipers OP, de Vos WM. Comparison of lantibiotic gene clusters and encoded proteins. Antonie van Leeuwenhoek. 1996; 69:171–184. [PubMed: 8775977]
5. Xie L, et al. Lacticin 481: *in vitro* reconstitution of lantibiotic synthetase activity. Science. 2004; 303:679–681. [PubMed: 14752162]
6. Bierbaum G, Sahl HG. Lantibiotics: mode of action, biosynthesis and bioengineering. Curr. Pharm. Biotechnol. 2009; 10:2–18. [PubMed: 19149587]
7. Cotter PD, Hill C, Ross RP. Bacterial lantibiotics: strategies to improve therapeutic potential. Curr. Protein Pept. Sci. 2005; 6:61–75. [PubMed: 15638769]
8. Chatterjee C, Paul M, Xie L, van der Donk WA. Biosynthesis and mode of action of lantibiotics. Chem. Rev. 2005; 105:633–684. [PubMed: 15700960]
9. Tang W, van der Donk WA. The sequence of the enterococcal cytolysin imparts unusual lanthionine stereochemistry. Nat. Chem. Biol. 2013; 9:157–159. [PubMed: 23314913]
10. Cox CR, Coburn PS, Gilmore MS. Enterococcal cytolysin: a novel two component peptide system that serves as a bacterial defense against eukaryotic and prokaryotic cells. Curr. Prot. Pept. Sci. 2005; 6:77–84.
11. Huycke MM, Spiegel CA, Gilmore MS. Bacteremia caused by hemolytic, high-level gentamicin-resistant *Enterococcus faecalis*. Antimicrob. Agents Chemother. 1991; 35:1626–1634. [PubMed: 1929336]
12. Libertin CR, Dumitru R, Stein DS. The hemolysin/bacteriocin produced by enterococci is a marker of pathogenicity. Diagn. Microbiol. Infect. Dis. 1992; 15:115–120. [PubMed: 1572135]
13. Chow JW, et al. Plasmid-associated hemolysin and aggregation substance production contribute to virulence in experimental enterococcal endocarditis. Antimicrob. Agents Chemother. 1993; 37:2474–2477. [PubMed: 8285637]
14. McClerren AL, et al. Discovery and in vitro biosynthesis of haloduracin, a two-component lantibiotic. Proc. Natl. Acad. Sci. U.S.A. 2006; 103:17243–17248. [PubMed: 17085596]
15. Shi Y, Yang X, Garg N, van der Donk WA. Production of lantipeptides in *Escherichia coli*. J. Am. Chem. Soc. 2011; 133:2338–2341. [PubMed: 21114289]
16. Liu W, Chan AS, Liu H, Cochrane SA, Vederas JC. Solid supported chemical syntheses of both components of the lantibiotic lacticin 3147. J. Am. Chem. Soc. 2011; 133:14216–14219. [PubMed: 21848315]
17. Suda S, Cotter PD, Hill C, Ross RP. Lacticin 3147- biosynthesis, molecular analysis, immunity, bioengineering and applications. Curr. Protein Pept. Sci. 2012; 13:193–204. [PubMed: 21827422]
18. Li B, et al. Catalytic promiscuity in the biosynthesis of cyclic peptide secondary metabolites in planktonic marine cyanobacteria. Proc. Natl. Acad. Sci. U.S.A. 2010; 107:10430–10435. [PubMed: 20479271]
19. Tang W, van der Donk WA. Structural characterization of four prochlorosins: a novel class of lantipeptides produced by planktonic marine cyanobacteria. Biochemistry. 2012; 51:4271–4279. [PubMed: 22574919]

20. Zhang Q, Yu Y, Velásquez JE, van der Donk WA. Evolution of lanthipeptide synthetases. Proc. Natl. Acad. Sci. U. S. A. 2012; 109:18361–18366. [PubMed: 23071302]
21. Bindman NA, van der Donk WA. A general method for fluorescent labeling of the N-termini of lanthipeptides and its application to visualize their cellular localization. J. Am. Chem. Soc. 2013; 135:10362–10371. [PubMed: 23789944]
22. Michelson AZ, et al. Gas-phase studies of substrates for the DNA mismatch repair enzyme MutY. J. Am. Chem. Soc. 2012; 134:19839–19850. [PubMed: 23106240]
23. Zu L, et al. Effect of isotopically sensitive branching on product distribution for pentalenene synthase: support for a mechanism predicted by quantum chemistry. J. Am. Chem. Soc. 2012; 134:11369–11371. [PubMed: 22738258]
24. Zanuy D, Casanovas J, Alemán C. The conformation of dehydroalanine in short homopeptides: molecular dynamics simulations of a 6-residue chain. Biophys. Chem. 2002; 98:301–312. [PubMed: 12128182]
25. Mathur P, Ramakumar S, Chauhan VS. Peptide design using alpha,beta-dehydro amino acids: from beta-turns to helical hairpins. Biopolymers. 2004; 76:150–161. [PubMed: 15054895]
26. Krenske EH, Petter RC, Zhu Z, Houk KN. Transition states and energetics of nucleophilic additions of thiols to substituted alpha,beta-unsaturated ketones: substituent effects involve enone stabilization, product branching, and solvation. J. Org. Chem. 2011; 76:5074–5081. [PubMed: 21574592]
27. Lohans CT, Li JL, Vederas JC. Structure and biosynthesis of carnolysin, a homologue of enterococcal cytolysin with D-amino acids. J. Am. Chem. Soc. 2014; 136:13150–13153. [PubMed: 25207953]
28. Zhou H, et al. A fungal ketoreductase domain that displays substrate-dependent stereospecificity. Nat. Chem. Biol. 2012; 8:331–333. [PubMed: 22406519]
29. May O, Nguyen PT, Arnold FH. Inverting enantioselectivity by directed evolution of hydantoinase for improved production of L-methionine. Nat. Biotechnol. 2000; 18:317–320. [PubMed: 10700149]
30. Turner NJ. Controlling chirality. Curr. Opin. Biotechnol. 2003; 14:401–406. [PubMed: 12943849]
31. Mugford PF, Wagner UG, Jiang Y, Faber K, Kazlauskas RJ. Enantiocomplementary enzymes: classification, molecular basis for their enantiopreference, and prospects for mirror-image biotransformations. Angew. Chem. Int. Ed. 2008; 47:8782–8793.
32. Reetz MT. Laboratory evolution of stereoselective enzymes: a prolific source of catalysts for asymmetric reactions. Angew. Chem. Int. Ed. 2011; 50:138–174.
33. Mukherjee S, van der Donk WA. Mechanistic studies on the substrate-tolerant lanthipeptide synthetase ProcM. J. Am. Chem. Soc. 2014; 136:10450–10459. [PubMed: 24972336]
34. Garg N, Tang W, Goto Y, Nair SK, van der Donk WA. Lantibiotics from *Geobacillus thermodenitrificans*. Proc. Natl. Acad. Sci. U.S.A. 2012; 109:5241–5246. [PubMed: 22431611]
35. Wang J, Wolf RM, Caldwell JW, Kollman PA, Case DA. Development and testing of a general amber force field. J. Comput. Chem. 2004; 25:1157–1174. [PubMed: 15116359]
36. Bayly CI, Cieplak P, Cornell WD, Kollman PA. A well-behaved electrostatic potential based method using charge restraints for deriving atomic charges: the RESP model. J. Phys. Chem. 1993; 97:10269–10280.
37. Darden T, York D, Pedersen L. Particle mesh Ewald: an N-log(N) method for Ewald sums in large systems. J. Chem. Phys. 1993; 98:10089–10092.
38. Hamelberg D, Mongan J, McCammon JA. Accelerated molecular dynamics: a promising and efficient simulation method for biomolecules. J. Chem. Phys. 2004; 120:11919–11929. [PubMed: 15268227]
39. Pierce LC, Salomon-Ferrer RF, de Oliveira CA, McCammon JA, Walker RC. Routine access to millisecond time scale events with accelerated molecular dynamics. J. Chem. Theory Comput. 2012; 8:2997–3002. [PubMed: 22984356]
40. Chai JD, Head-Gordon M. Long-range corrected hybrid density functionals with damped atom-atom dispersion corrections. Phys. Chem. Chem. Phys. 2008; 10:6615–6620. [PubMed: 18989472]
41. Zhao Y, Truhlar DG. The M06 suite of density functionals for main group thermochemistry, thermochemical kinetics, noncovalent interactions, excited states, and transition elements: two

new functionals and systematic testing of four M06-class functionals and 12 other functionals. Theor. Chem. Acc. 2008; 120:215–241.

42. Scalmani G, Frisch MJ. Continuous surface charge polarizable continuum models of solvation. I. General formalism. J. Chem. Phys. 2010; 132:114110. [PubMed: 20331284]

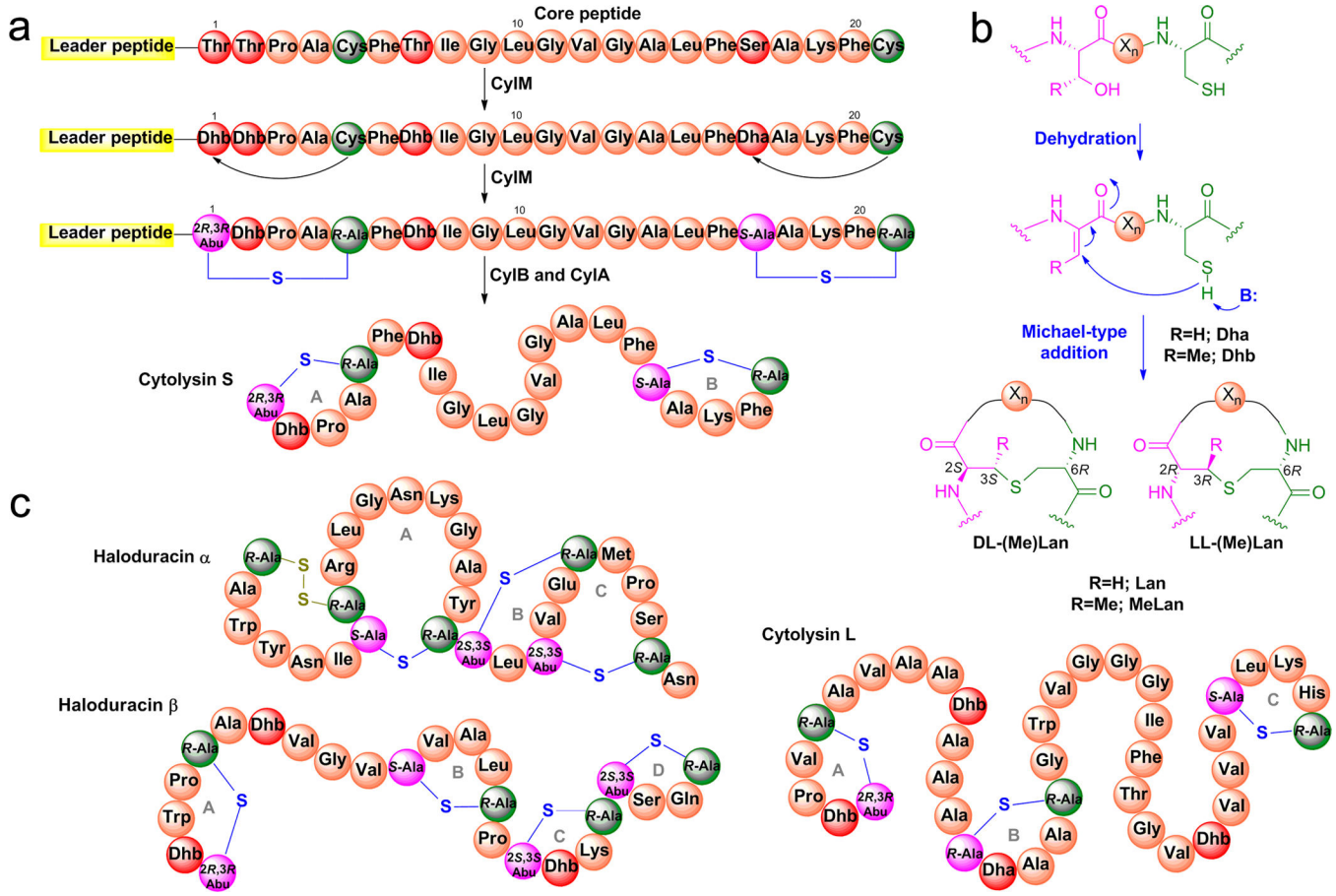

Figure 1. Biosynthesis of class II lanthipeptides

(a) Generic pathway of class II lanthipeptide biosynthesis with cytolysin S as an example. The $CylL_S$ peptide is synthesized by the ribosome as a linear precursor peptide with an N-terminal leader peptide and a C-terminal core peptide. The dehydration of Ser and Thr residues to Dha and Dhb residues as well as the Michael-type addition by Cys residues onto these α,β-unsaturated amino acids is catalyzed by the bi-functional lanthionine synthetase CylM. The leader peptide is then removed by the proteases CylB and CylA, affording mature cytolysin S. **(b)** Dehydration and cyclization reactions catalyzed by LanM enzymes that result in (Me)Lan residues with the canonical DL (i.e. D configuration at the α carbon originating from Ser or Thr and L configuration at the α carbon of the former Cys) and unusual LL (L configuration for both α carbons) stereochemistries. **(c)** The structures of haloduracin (Halα and Halβ) and cytolysin L. Abu, α-aminobutyric acid.

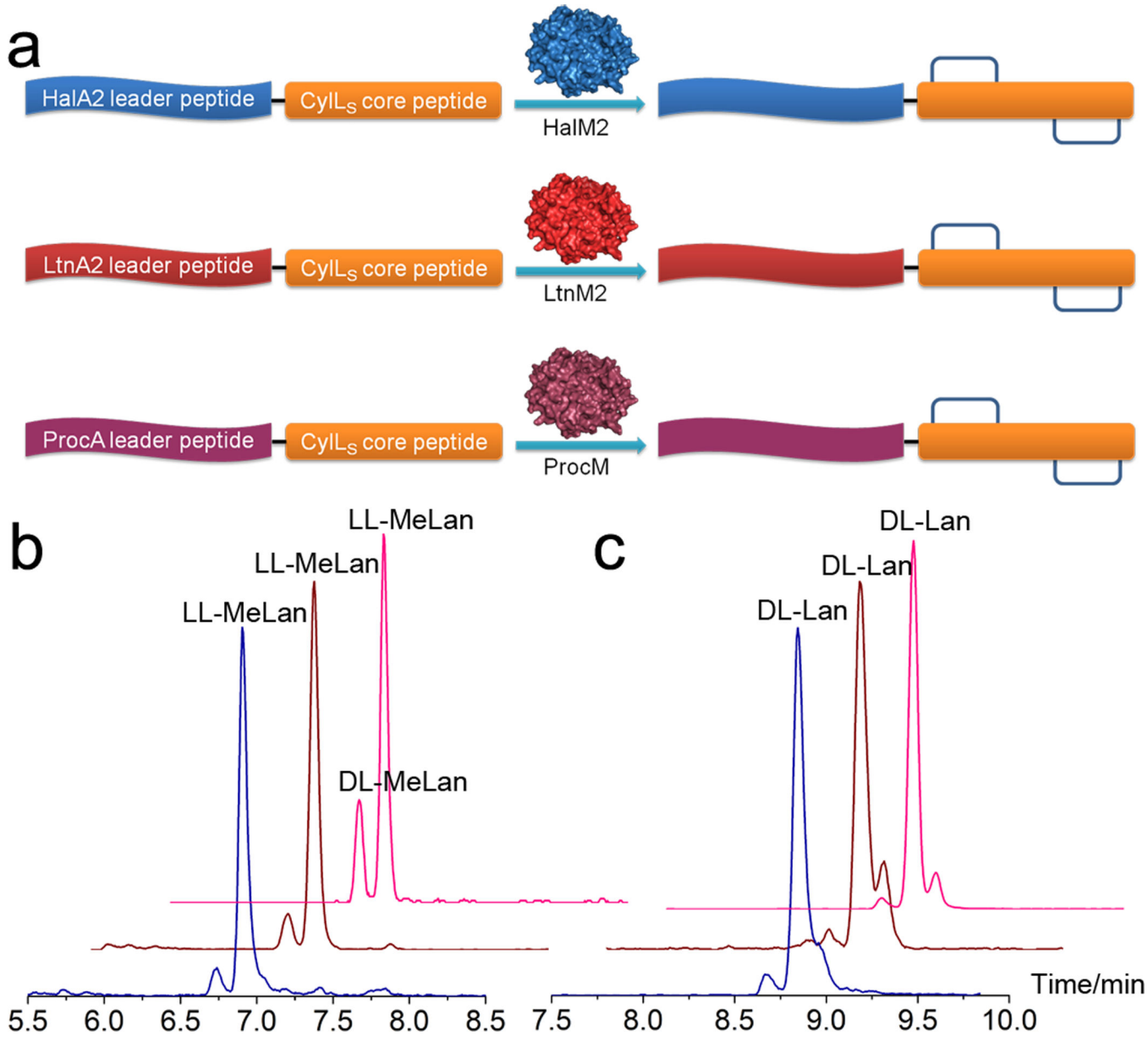

Figure 2. GC-MS analysis of *in vivo* modified HalA2-CylL$_S$, LtnA2-CylL$_S$ and ProcA3.2-CylL$_S$ chimeric peptides

(a) HalA2-CylL$_S$, LtnA2-CylL$_S$ and ProcA3.2-CylL$_S$ chimeras that were modified in *E. coli* by the lanthionine synthetases HalM2, LtnM2, and ProcM, respectively. A generic protein structure is shown for the three enzymes. GC-MS traces are shown for hydrolyzed and derivatized MeLan residues **(b)** and Lan residues **(c)** from modified HalA2-CylL$_S$ (blue), LtnA2-CylL$_S$ (red), and ProcA3.2-CylL$_S$ (magenta). All intensities were normalized with respect to the predominant product. For co-injection traces with synthetic (Me)Lan standards, see Supplementary Fig. S2, S4 and S7.

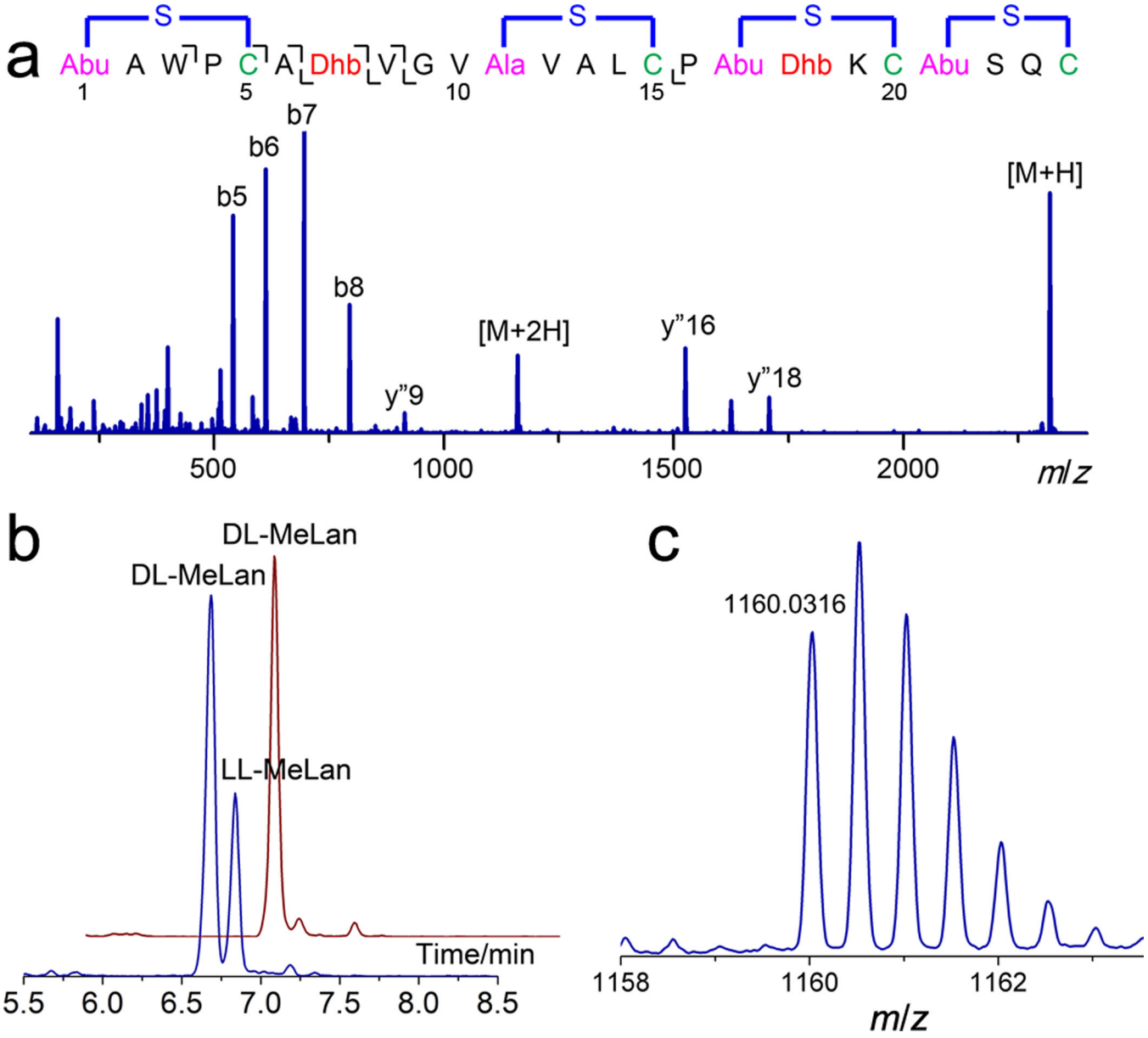

Figure 3. Structural characterization of HalM2-modified HalA2-T2A peptide

(a) MS/MS analysis of the HalA2-T2A core peptide modified by HalM2 in *E. coli*. Fragmentation is suppressed in the sequences spanning residues 1–5, 11–15, 17–20 and 21–24 as a result of ring formation. The b3 ion is attributed to in-ring fragmentation, which is rare but has also been observed for cytolysin, nisin and geobacillin[9,15,34]. **(b)** GC-MS traces for hydrolyzed and derivatized MeLan residues from HalM2-modified HalA2 peptide (blue) and HalM2-modified HalA2-T2A peptide (red). For co-injection traces of hydrolyzed and derivatized (Me)Lan residues obtained from modified HalA2-T2A peptide with synthetic (Me)Lan standards, see Supplementary Fig. S8. **(c)** Electrospray ionization (ESI) quadrupole TOF mass spectrum for modified HalA2-T2A core peptide. The $[M+2H]^{2+}$ ion was observed with an *m/z* value of 1160.0316 (calculated *m/z* of cyclized HalA2-T2A core peptide with 2 protons: 1160.0313).

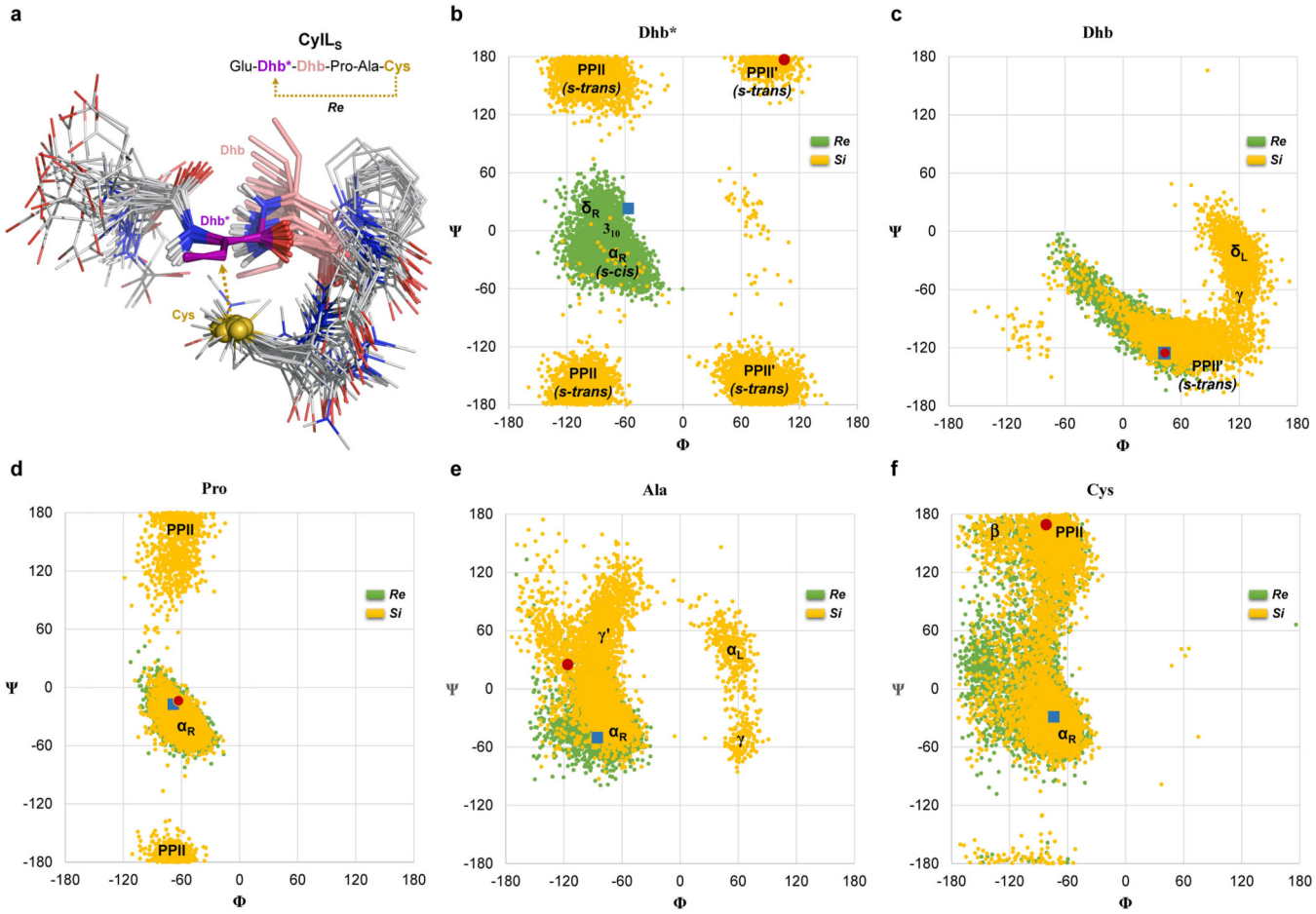

Figure 4. Secondary structure of the A ring of the CylL$_S$ core sequence derived from MD simulations

(a) Overlay of 20 representative conformers obtained from the accelerated MD (aMD) trajectory restrained to the *Re* face approach. **(b–f)** Ramachandran plots obtained through the simulations for the five residues involved in the macrocyclization. The lowest energy QM optimized transition structures for both approximations are shown as blue squares (*Re*) and red circles (*Si*). The higher rigidity of the peptide backbone in the most stable *Re* face approach is apparent. Also, MD simulations show a change in the conformation of the reactive Dhb from α-helical (*s-cis*) to PPII (*s-trans*) in the *Si* face approach, while the remaining amino acids qualitatively preserve the same conformation.

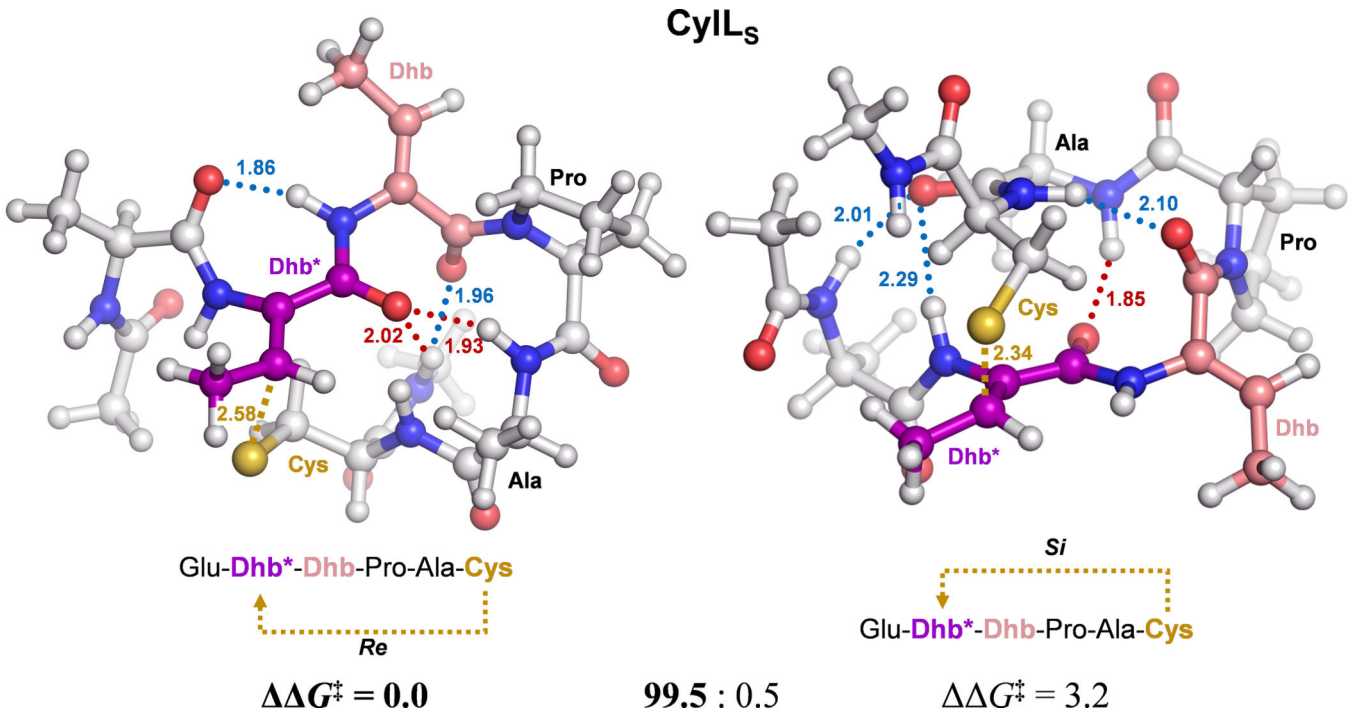

Figure 5. Lowest energy quantum mechanical transition structures for the *Re* and *Si* face Michael-type additions that generate the A ring in the CylL$_S$ core sequence

Geometries were optimized at the IEF-PCM/ω-B97X-D/6-31G(d) level and the relative activation free energies ($\Delta\Delta G^{\ddagger}$, in kcal mol^{-1}) were calculated at the IEF-PCM/M06-2X/6-311+G(2d,p) level. The depicted kinetic diastereomeric percentage was derived from these relative activation energies. The presence of a tight hydrogen bond network in the *Re* face approach, which creates a rigid oxyanion hole to stabilize the developing negative charge on the carbonyl oxygen, stabilizes this transition state significantly and favors *Re*-face attack to occur almost exclusively.

Table 1

Stereochemical outcome of lanthipeptide precursor peptides modified by different lanthionine synthetases.

Peptide substrate	Lanthionine synthetase	Configuration of (Me)Lan residue		Quantum mechanical prediction for A ring
		A ring[a]	Other rings	
$CylL_S$	CylM[b]	LL	DL	LL
HalA2-$CylL_S$	HalM2	LL	DL	LL
LtnA2-$CylL_S$	LtnM2	LL	DL	LL
ProcA3.2-$CylL_S$	ProcM	LL	DL	LL
HalA2	HalM2[b]	LL	DL	LL
HalA2-T2A	HalM2	DL	DL	DL

[a] The ring that contains the Dhb-Dhb-Xxx-Xxx-Cys motif.

[b] Reported previously[9].